Cell, Vol. 76, 427–437, February 11, 1994, Copyright © 1994 by Cell Press

141

Whisker-Related Neuronal Patterns Fail to Develop in the Trigeminal Brainstem Nuclei of NMDAR1 Knockout Mice

Yuqing Li,* Reha S. Erzurumlu,† Chong Chen,* Sonal Jhaveri,† and Susumu Tonegawa*
*Howard Hughes Medical Institute
at the Center for Cancer Research
and Department of Biology
Massachusetts Institute of Technology
Cambridge, Massachusetts 02139
†Department of Brain and Cognitive Sciences
Massachusetts Institute of Technology
Cambridge, Massachusetts 02139

Summary

Sensory pathways of the brain generally develop from crudely wired networks to precisely organized systems. Several studies have implicated neural activity–dependent mechanisms, including N-methyl-D-aspartate (NMDA) receptors, in this refinement process. We applied the gene targeting to the *NMDAR1* gene and created a mutant mouse that lacks functional NMDA receptors. The development of whisker-related patterns in the trigeminal nuclei of the mutant mice and their normal littermates was compared. We show that in the mutant mice pathfinding, initial targeting, and crude topographic projection of trigeminal axons in the brainstem are unaffected, but that whisker-specific patches fail to form. Our results provide a direct demonstration of the involvement of the NMDA receptor in the formation of periphery-related neural patterns in the mammalian brain.

Introduction

In most sensory systems, the periphery is mapped in a topographic fashion onto multiple cell groups in the brain. Studies of the mechanisms involved in the development of such maps have focused on the visual system, and have implicated a key role for NMDA receptor–mediated activity in the refinement of topographic maps. Thus, N-methyl-D-aspartate (NMDA) receptors have been implicated in the formation of eye-specific stripes in the frog tectum (Cline et al., 1987), topographic segregation of retinocollicular afferent arbors in the rat (Simon et al., 1992), the formation of so called On and Off sublaminae in ferret lateral geniculate nucleus (Hahm et al., 1991), and the plasticity of ocular dominance columns in the cat visual cortex (Kleinschmidt et al., 1987; Bear et al., 1990). The prevailing hypothesis states that correlated activity in afferents that converge on specific neurons results in depolarization of the postsynaptic membrane via non-NMDA receptors and removal of the magnesium block on NMDA receptors. This allows the glutamate released by subsequent action potentials to open the NMDA receptor channel; Ca^{++} enters into the postsynaptic cell, and triggers the activation of second messenger systems. The resulting cascade of events succeeds (via unknown mechanisms) in providing feedback to the presynaptic fibers, leading to consolidation of synaptic connections associated with fibers that fire in synchrony. In contrast, connections made by axons that do not fire in synchrony are weakened by virtue of their inability to activate the NMDA receptors and their failure to trigger the subsequent cascade of events in postsynaptic cells (for reviews see Constantine-Paton et al., 1990; Shatz, 1990).

The whisker-to-barrel system of common laboratory rodents is highly suitable for the study of mechanisms underlying sensory map formation. Tactile hairs (whiskers and sinus hairs) on the snout are arranged in a discrete array and collectively form a unique sense organ that is important for the exploratory behavior of the animal. Peripheral and central processes of the trigeminal ganglion connect the whisker pad to the brain. Central axon arbors of trigeminal ganglion cells and their postsynaptic target neurons replicate the whisker pattern in three distinct nuclei of the brainstem trigeminal complex (BSTC). The neuronal pattern is first established in the brainstem, which then provides a template for whisker-related patterns seen in the dorsal thalamus and in the primary somatosensory cortex, or barrel cortex (schematized in Figure 1; also reviewed by Woolsey, 1990; Jhaveri and Erzurumlu, 1992).

The role of activity, NMDA receptors, or both in the development of the whisker-to-barrel system has been studied using activity blockers, such as TTX or AP5, applied either to the branch of the trigeminal nerve that innervates the whiskers (Henderson et al., 1992) or directly to the barrel cortex in newborn rats (Chiaia et al., 1992c; Schlaggar et al., 1993). Although lesions of the sensory periphery dramatically alter whisker-related patterns in the brain within a few days of birth (Belford and Killackey, 1980; Jeanmonod et al., 1981; Durham and Woolsey, 1984), activity blockade experiments failed to prevent the emergence of these patterns. In addition, the low levels of spontaneous activity in the developing trigeminal system (Chiaia et al., 1993) have led to the suggestion that the development of whisker-related patterns may be established independent of activity (Chiaia et al., 1992c, 1993; Henderson et al., 1993, 1994).

At least five subunits of NMDA receptors have been identified. Of these, the R1 subunit is essential for NMDA receptor activity (reviewed by Nakanishi, 1992). As a first step toward the genetic analysis of activity-dependent development and plasticity of sensory maps in the mammalian brain, we have used so called reverse genetics to selectively knock out (reviewed by Capecchi, 1989) the NMDAR1 subunit of the NMDA receptor. To reexamine the role of NMDA receptor–mediated activity in the establishment of neural patterns in the brainstem, those areas of the trigeminal nuclei that express whisker-specific patterns were compared in mutant and control animals. Our results show that in the knockout animals, although central targeting and topographic projection of the trigeminal afferents appear to be normal and postsynaptic neurons are responsive to stimulation of primary trigeminal afferents,

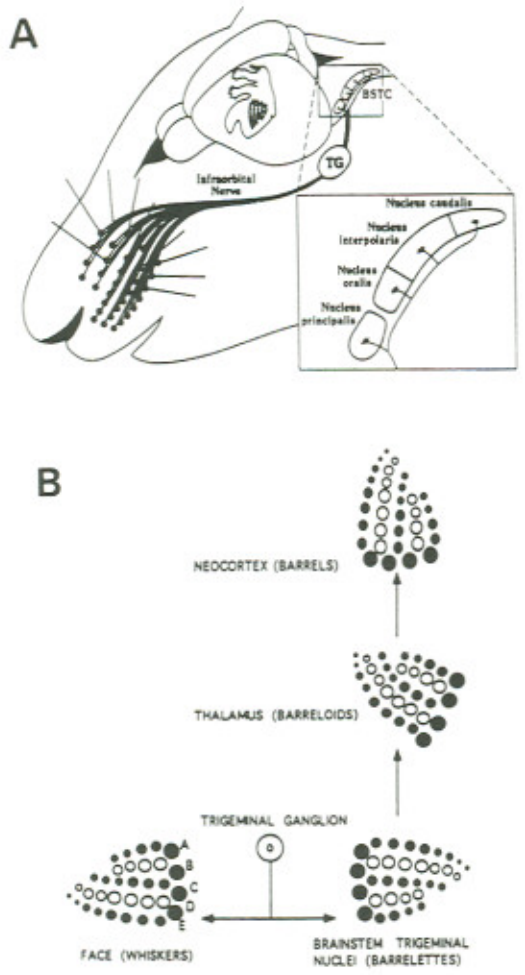

Figure 1. Rodent Whisker-to-Barrel System

(A) A population of trigeminal ganglion cells (TG) sends peripheral processes into the infraorbital nerve to innervate the whiskers; central processes of these cells project to BSTC. The BSTC consists of nucleus principalis and subnuclei oralis, interpolaris, and caudalis. Whisker-related patterns (barrelettes) are only present in nucleus principalis and subnuclei interpolaris and caudalis. In the cortex, the body surface representation as well as barrels (closed dots) are shown. To facilitate the visualization of the BSTC, the cerebellum is removed from the mouse brain in the drawing.

(B) Schematic drawing showing the whisker-specific neural patterns along the trigeminal pathway. Five rows (A–E) of whiskers are schematized on the face. This pattern is replicated by axonal and neuronal elements in the brainstem trigeminal nuclei (barrelettes), in the ventrobasal nucleus of the thalamus (barreloids), and in the primary somatosensory neocortex (barrels). While the whisker pattern is replicated in each of the trigeminorecipient brain region, the overall orientation of the pattern in each station is different.

whisker-specific neural patterns fail to develop in the absence of the NMDA receptor. These results lead us to challenge the view that whisker-related patterns are formed independent of neural activity.

Results

Generation of NMDAR1-Mutant Mice

Southern blot analysis of mouse genomic DNA with a DNA probe (encoding a sequence of about 100 amino acids of NMDAR1 polypeptide chain) detected only one band in each lane (BamHI, 1.1 kb; EcoRI, 19 kb; EcoRV, 5.4 kb; and HindIII, 15.4 kb), suggesting that *NMDAR1* gene is a single copy gene in the mouse genome. The *NMDAR1* targeting vector (Figure 2A) has a 2.5 kb homologous sequence on the 5′ side and a 8.3 kb sequence on the 3′ side. Upon homologous recombination, this construct removed a 2.4 kb region encoding 338 amino acids, including four transmembrane domains. The deleted region was replaced by a neomycin-resistance (*neo*) gene controlled by the phosphoglycerate kinase-1 (*pgk*) promoter. Clones resistant to G418 were screened for the desired homologous recombination event by Southern blotting. Blots were hybridized with a 3′ flanking probe and a 5′ internal probe. Of 251 clones analyzed, 8 carried the expected mutation. The results of one targeted clone and a wild-type control are shown in Figure 2B.

Embryonic stem (ES) cells of the targeted clones were injected into blastocysts, which were then implanted into foster mothers (Bradley, 1987). Chimeric animals from the first four clones injected were mated with C57BL/6 mice to test germline transmission. They all transmitted the mutation to their offspring. Heterozygous animals (F1) were bred to produce homozygous mutants (F2). Later, heterozygous animals of different inbred backgrounds were crossed to produce littermates (hybrid animals) for studies of the whisker-barrel system.

NMDAR1-Deficient Mice Die after Birth

Out of 177 F2 animals genotyped by Southern blot analysis at 3–4 weeks of age, 60 were found to be wild-type animals and the rest were heterozygous animals, indicating that the NMDAR1 deficiency is lethal. To determine the exact time when the homozygotes fail to survive, we analyzed mutants at various ages during embryonic and neonatal development, between embryonic day (E) 13 and P0 (E0, day of plug; P0, day of birth).

Until P0, the ratio of wild-type:heterozygotes:homozygotes is 25:41:22, close to 1:2:1; thus, the mutation does not result in embryonic fatality. However, about 10–20 hr after birth, the homozygotes are either thrown out of the nest unattended or are dead inside the nest. Visual inspection of normal (wild-type and heterozygous) newborn pups and homozygous pups showed that the mutant animals do not have milk in their stomachs, most likely owing to problems with their suckling reflexes. Moreover, the mutant animals are severely ataxic and cannot support their body weight on their hindlimbs.

The skin of the newborn mutant animals is flushed and has a reddish coloration, much like their wild-type littermates; thus, their cardiovascular and respiratory systems are functional at least soon after birth. No abnormality was detected in the electrocardiographic pattern or the respiratory rhythm of newborn mutant mice (X. Li, Y. L., C.-S. Poon, and S. T., unpublished data). However, increased apnea is observed within several hours of birth and cyanosis appears shortly before death (X. Li, Y. L., C.-S. Poon, and S. T., unpublished data). We interpret

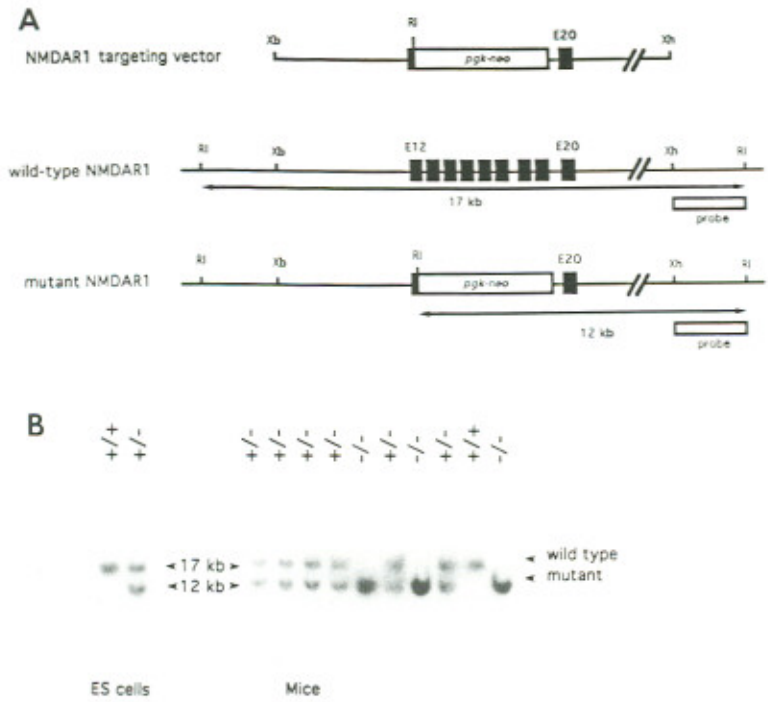

Figure 2. Production of NMDAR1-Mutant Mice

(A) The targeting construct, wild-type, and mutant loci for *NMDAR1*. The exon–intron structure of rat *NMDAR1* gene has been described (Hollmann et al., 1993). For the mouse *NMDAR1* gene, the position of introns is the same as for their rat counterparts, though the length of each individual intron differs slightly from rat sequence (unpublished data). The portion of the *NMDAR1* gene that includes exons 12–20 is shown. A 2.4 kb fragment from the *NMDAR1* gene was deleted and replaced with a *neo* gene. Closed boxes represent *NMDAR1* exon sequences. *NMDAR1* 3′ flanking probe used for screening of ES cell clones and mutant mice is indicated, together with the expected size of hybridizing restriction fragments in wild-type and mutant *NMDAR1* alleles (also see [B]). Abbreviations for restriction enzyme sites: Xb, XbaI; RI, EcoRI; Xh, XhoI.

(B) Southern blot analysis of a representative ES cell clone and tail biopsies. Genomic DNA was isolated from an ES cell clone with a mutated *NMDAR1* allele (+/-) and a wild-type control (left, +/+), and from a litter of 10 pups resulting from a heterozygous (+/-) intercross (right). DNA was digested with EcoRI and hybridized with 3′ flanking probe (see Figure 2A). Wild-type and mutant alleles are indicated. Three mice in the litter are homozygous (-/-) for the mutation.

these observations to mean that respiratory failure contributes to mutant animal fatality.

At the time of birth, the mutant animals are responsive to hypercapnia: respiration is increased in frequency and in depth at high concentration of CO_2, which demonstrates that the respiratory control in response to CO_2 levels is intact in these animals (X. Li, Y. L., C.-S. Poon, and S. T., unpublished data). We took advantage of this ability in attempts to prolong the life of the mutants by stimulating their respiration with CO_2. In addition, pregnant mothers were injected with terbutaline, a β-adrenergic agonist, every 4–6 hr starting at E18.5. This usually delayed birth for 1 day. Treated animals were then allowed to give birth. Newborn pups were weighed and put into an air incubator. They were monitored closely. If cyanosis was observed, they were treated in a CO_2 chamber to stimulate respiration. Wild-type or heterozygous littermate controls were treated according to the same regimen.

The average body weight for mutant pups at the time of birth is 1.323 ± 0.130 g (n = 10), close to that of wild-type and heterozygous animals (1.321 ± 0.171 g; n = 11), indicating that the general development of the knockout mice is not significantly perturbed in utero.

Absence of Whisker-Related Patterns in the Brainstem Trigeminal Complex of Mutant Mice

In the brain of the normal mouse, the five rows (A–E) of whiskers, with specific numbers of whisker follicles in each row, are conspicuously represented by discrete neuronal modules in several trigeminorecipient zones (for reviews see Woolsey, 1990; Van der Loos and Welker, 1985). In the brainstem trigeminal nuclei, the whisker-specific modules (barrelettes) are composed of the arbors of trigeminal sensory axons and the postsynaptic cells to which these axons project (Bates and Killackey, 1985; Ma, 1991). These neural elements form cylindrical aggregates oriented along the rostro–caudal axis of the brainstem. In transverse sections stained for mitochondrial enzymes (e.g., cytochrome oxidase [CO] or succinic dehydrogenase), five distinct rows of patches can be identified, each patch corresponding to a single whisker or sinus hair (Belford and Killackey, 1979; Ma and Woolsey, 1984). It is noteworthy that while patches of mitochondrial enzyme activity are closely correlated with the patterning of presynaptic axon arbors (Bates and Killackey, 1985; Chiaia et al., 1992a), reactive mitochondria are located primarily in the dendrites and somata of postsynaptic cells (Chiaia et al., 1992b). Thus, CO patterns in the brainstem can be taken as a reliable marker of the aggregation of postsynaptic neurons into barrelettes. The complete whisker-related pattern is repeated several times in the hindbrain: once in the principal sensory nucleus and once each in the subnuclei interpolaris and caudalis of the spinal trigeminal nucleus.

Animals with the genetic background we have used, namely, 129/Sv × BALB/c, C57BL/6 × BALB/c, or C57BL/6 × 129/Sv, are born between E18.5 and E19.5 (we refer to the morning of E19 as P0). In wild-type as well as in heterozygous animals of these strains, CO histochemistry reveals an emerging segmentation of the reaction product at the earliest time (E18.5) that the mice are born (Figure 3A). This is a day prior to that previously reported for Swiss–Webster outbred mice (Ma, 1993). We attribute this difference in emergence of the barrelettes to strain-dependent variations. In all our wild-type (n = 4) and het-

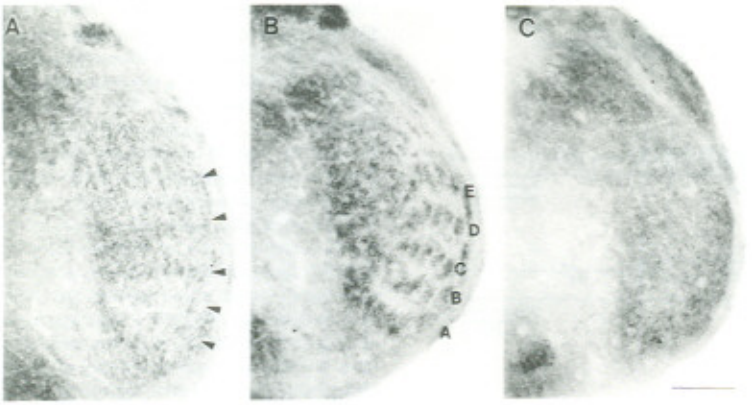

Figure 3. Coronal Sections through the Brainstem at the Level of Subnucleus Interpolaris

Sections are stained for visualization of the mitochondrial enzyme cytochrome oxidase.

(A) Normal control animal, aged E18.5. Differentiation of the five whisker rows is just beginning at this age in animals with the genetic background we have used in this study. Arrowheads point to the five rows. Dorsal is up in each micrograph, lateral is to the right.

(B) Wild-type control animal, age P2. This pup was removed from the mother at the time of birth and placed in an air incubator, along with its mutant littermate. In the normal animal, individual whisker-specific patches within the five whisker rows (A–E) are clearly discernible.

(C) Subnucleus interpolaris of mutant mouse lacking the gene for the NMDAR1 receptor. This animal was kept alive, along with a wild-type littermate, as described for (B). Even at an age equivalent to P2, no whisker-specific cytochrome oxidase–positive pattern is visible in the mutant animal. Scale bar, 0.2 mm for all three sections.

erozygous animals (n = 3), individual barrelettes are readily discernible by late P0 (E19.5). However, in none of the mutant animals (n = 9) is there any indication of row or patch formation.

To rule out the possibility of developmental retardation in the mutant animals, terbutaline was used to block the birth of mutant as well as normal pups in several litters. In combination, we attempted to extend the life of the mutant animals by CO_2 stimulation after birth. Normal littermate pups were treated the same way as controls were. These measures allowed the mutants to survive up to 21 days after conception (equivalent to P2; n = 3). Figure 3B shows a section through the spinal trigeminal nucleus of a wild-type pup whose birth was delayed for 1 day and that was kept in an incubator for an additional day (equivalent to P2). CO-positive barrelettes are clearly visible in this case, while no evidence of rows or individual patches is noted in the mutant littermate that survived to P2 under the same conditions (Figure 3C). This is true for all levels of the BSTC. Figure 4 illustrates that at P1.5, wild-type pups (n = 7) have normal barrelettes in principal nucleus and in subnuclei interpolaris and caudalis of the spinal

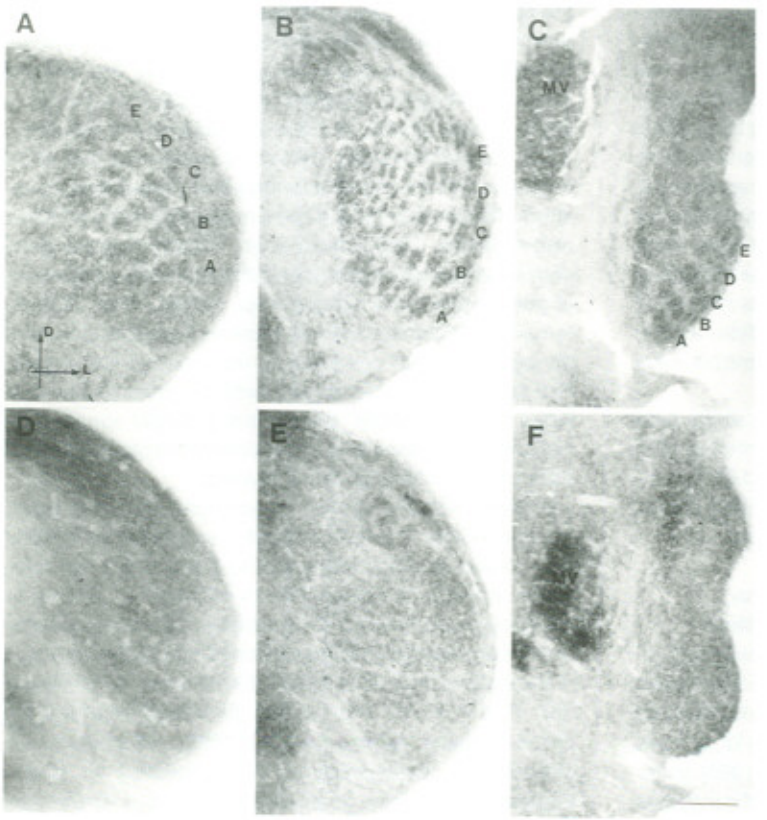

Figure 4. Cytochrome Oxidase–Stained Sections in Wild-Type and Mutant Animals, both Aged P1.5

Wild-type animals are shown in the top row; mutants are shown in the bottom row. Sections are shown at the level of subnucleus caudalis (A, D), and interpolaris (B, E) of the spinal trigeminal nucleus, and also at the level of nucleus principalis (C, F). Individual barrelettes are visible within the five whisker row representations (A–E) at all three levels of the brainstem trigeminal complex in the normal animal, whereas they are lacking at all three levels in the knockout mouse. MV, motor nucleus of the trigeminal nucleus. Cytochrome oxidase staining in MV is dense, both in control and mutant animals, indicating that failure of pattern formation in the mutants is not merely a reflection of the general absence of cytochrome oxidase activity throughout the brain. D, dorsal; L, lateral for all micrographs. Scale bar, 0.2 mm for all six micrographs.

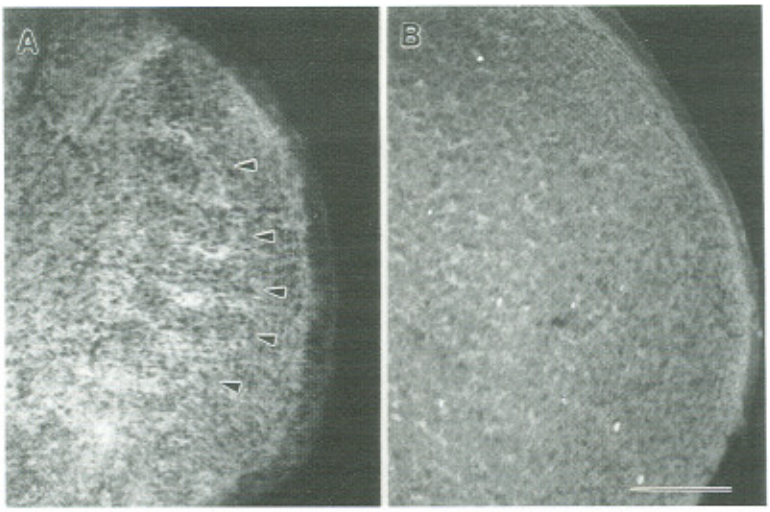

Figure 5. Barrelettes Detected by Immunohistochemistry for CTBP

Coronal sections through the brainstem of normal (A) and mutant (B) P0 mice at the level of subnucleus interpolaris. The sections were immunostained with an antibody against the extracellular matrix molecule CTBP. The immunopositive pattern in the brainstem of the normal control animal reflects the emerging pattern of barrelettes. Note that the proteoglycan is deposited in the regions between rows. The five whisker-specific rows are indicated by arrowheads. No emergent pattern can be discerned with this antibody along the BSTC of the mutant animal. Scale bar, 0.2 mm for both micrographs.

trigeminal nucleus, while their knockout littermates (n = 4) do not have these patterns. This difference cannot be attributed to a general lack or greatly diminished expression of the CO enzyme in the mutant brain: levels of CO enzymatic activity appear to be normal in regions of the hindbrain such as the hypoglossal nuclei, the inferior olive, and the motor nucleus of the trigeminal nerve. In addition, although the CO-positive patches are not visible in the trigeminal nuclei, a staining above background levels does exist in this region (see Figure 3C; Figure 4).

The lack of barrelette formation in knockout animals was confirmed with the use of an alternative marker for delineating barrelette boundaries. Brainstem sections from normal and mutant mice were stained immunohistochemically, using a polyclonal antibody directed against cytotactin-binding proteoglycan (CTBP). CTBP is an extracellular matrix molecule secreted by neurons. Its distribution reveals whisker-specific patterns along the trigeminal pathway (Crossin et al., 1989; Jhaveri et al., 1991). Unlike the CO activity pattern, CTBP is distributed around individual barrelettes, thus giving an image that is complementary to the pattern seen with CO histochemistry. Figure 5 shows an emergent segmented pattern in a CTBP-immunostained coronal section through the BSTC of a wild-type pup on P0 (Figure 5A; n = 5) and the lack of any pattern in an age-matched mutant pup (Figure 5B; n = 4). Together with the absence of CO patches, these observations confirm that barrelettes do not form in the mice that lack functional NMDA receptors.

Development of the Trigeminal Pathway in Normal and Mutant Mice

On P0, the gross appearance of the whiskers and their arrangement into five rows (A–E) is normal in the mutant mice. To determine that the absence of barrelettes does not result from a delayed connectivity between the whisker pad and the BSTC, we compared the development of the peripheral trigeminal pathway in control and mutant animals. Immunohistochemical staining using an antibody (TuJ1) against neuron-specific β-tubulin in E11 embryos

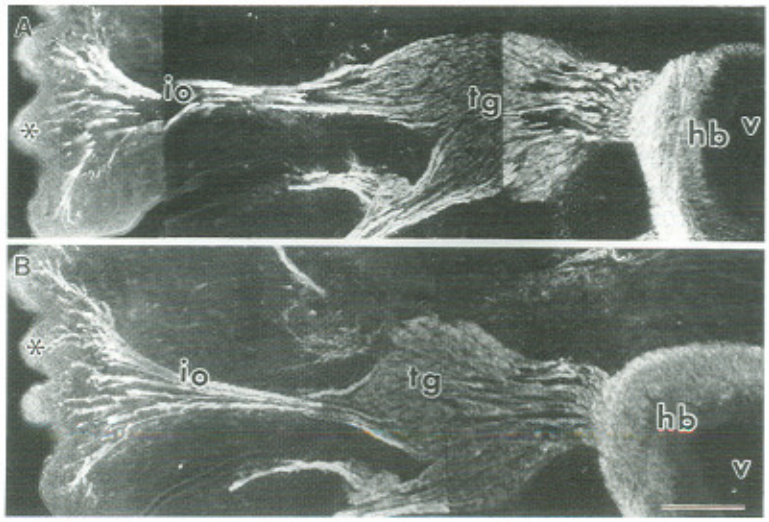

Figure 6. Absence of Whisker-Specific Patterns in Mutant Animals Is Not Due to a Delay in the Establishment of Trigeminal Connections between the Whisker Pad and the Brainstem

The first trigeminal axons in the mouse reach the presumptive whisker pad on E10 (Stainier and Gilbert, 1990). On E11, immunostaining for neuron-specific β-tubulin (using the TuJ1 antibody) reveals that, both in the normal (A) and in the mutant (B) animals, peripheral trigeminal axons have fully invaded the developing whisker pad. Central trigeminal axons have entered the hindbrain. No significant differences can be distinguished in the size of the trigeminal ganglion or of the trigeminal nerve between the mutant and normal animals. io, infraorbital nerve; tg, trigeminal ganglion; hb, hindbrain; v, ventricle; *, presumptive whisker pad. Scale bar, 0.3 mm.

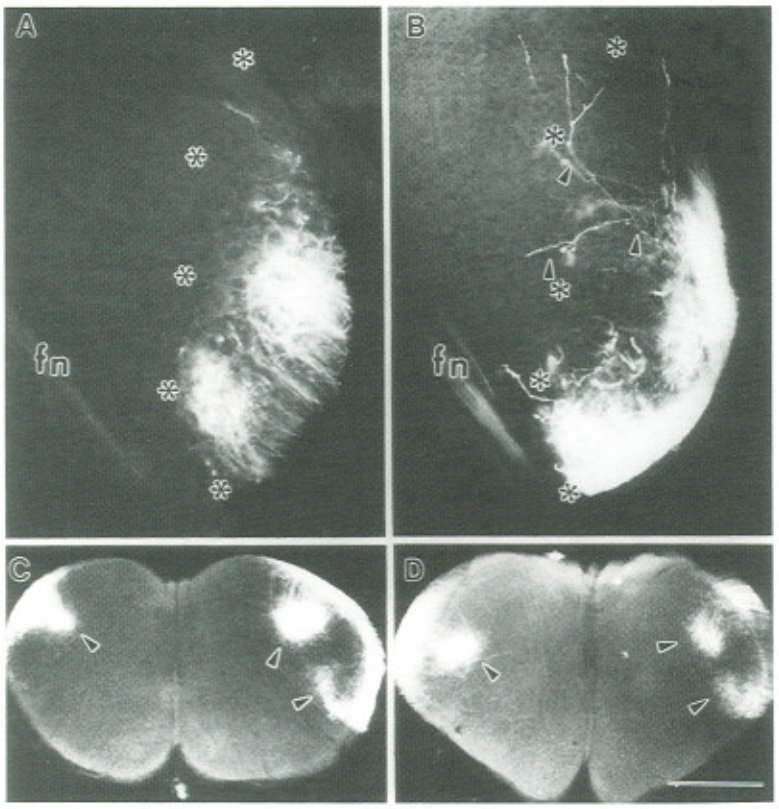

Figure 7. Spatial Order of Trigeminal Projections to Brainstem Nuclei

High magnification (A, B) and lower power (C, D) photomicrographs of coronal sections through the brainstem at the level of nucleus principalis (A, B) and subnucleus caudalis (C, D). All animals were sacrificed on the day of birth (P0). Tiny crystals of the dye DiI were placed in the dorsal whisker row (A) and ventral whisker row (E) on the right side of each animal, whereas a single crystal was placed on the middle row (C) on the left side. Discrete patches of DiI-labeled axonal arbors, which correspond to the labeled whiskers are detected in both the normal (A, C) and mutant (B, D) mice, demonstrating that the trigeminal projections are topographically organized in the mutant mouse. Asterisks in (A) and (B) indicate approximate boundaries of the nucleus principalis. fn, facial nerve. Arrowheads in (B) indicate a single axon arbor. Arrowheads in (C) and (D) show axonal patches stained by DiI from whisker pad. Scale bar, 0.2 mm for (A) and (B); 0.8 mm for (C) and (D).

revealed that trigeminal axons reach their peripheral and central targets at the same time, both in mutants (n = 4) and in controls (n = 6; Figure 6; cf. Stainier and Gilbert, 1990), and that there are no gross differences in the size of the trigeminal ganglion, or in the density of its projections, between the two types of animals.

Next, we applied nonoverlapping crystals of the lipophilic tracer DiI in the dorsal (A) and ventral (E) whisker rows on one side of the snout, and in the middle whisker row (C) on the opposite side, in normal (n = 12) and mutant mice (n = 12) that were killed and fixed on E17 or on P0. Following appropriate times to allow for the diffusion of the dye, patterns of axonal labeling in the BSTC were examined. In normal mice, as for rats (Erzurumlu and Jhaveri, 1992), this labeling technique reveals the spatial order of trigeminal ganglion cell processes (Figure 7). DiI labeling of the dorsal and ventral rows resulted in two patches of axonal labeling, both in the ipsilateral principal nucleus and in the spinal trigeminal nucleus. On the other side of the hindbrain, DiI labeling from the middle whisker row revealed a single patch of axonal labeling in the midregion of these same nuclei (Figure 7). Such topographic ordering is present in the central trigeminal projections of both mutant and normal mice. Moreover, the density of axonal arbors in the mutant animals did not appear to be compromised. In fact, the labeled patches appeared to be larger, and at least some axon arbors were more extensive in the mutant (Figure 7B). However, further quantitation of axonal arbors needs to be done and the extent of labeling in BSTC should be normalized with the spread of DiI in the whisker pad.

NMDAR1 Is Expressed at the Time of Barrelette Formation

To further investigate the involvement of NMDA receptors in the formation of barrelettes, we used sense and antisense probes for the NMDAR1 mRNA to perform in situ hybridization. The antisense RNA probe was incubated with coronal sections of both adult and newborn normal mice. The densely distributed grains observed with the antisense probe indicate the presence of high levels of the messenger for NMDAR1 in this part of the brainstem in the trigeminal nuclei of newborn mice (Figure 8A), while the sense probe showed no hybridization (Figure 8B). In adult mice, both neocortex and hippocampus gave strong hybridization signals, a pattern expected from previous studies (Figure 8C; cf. Moriyoshi et al., 1991). These results document that the messenger for the NMDAR1 subunit is present in the trigeminal nuclei of normal mice around the time of formation of the whisker-related patterns.

Excitability of Brainstem Trigeminal Neurons and Synaptic Transmission

To investigate whether NMDAR1 mRNA is translated and forms functional NMDA receptors in BSTC of normal newborn mice, and to study how the inactivation of NMDAR1 protein affects NMDA receptor–mediated and overall neu-

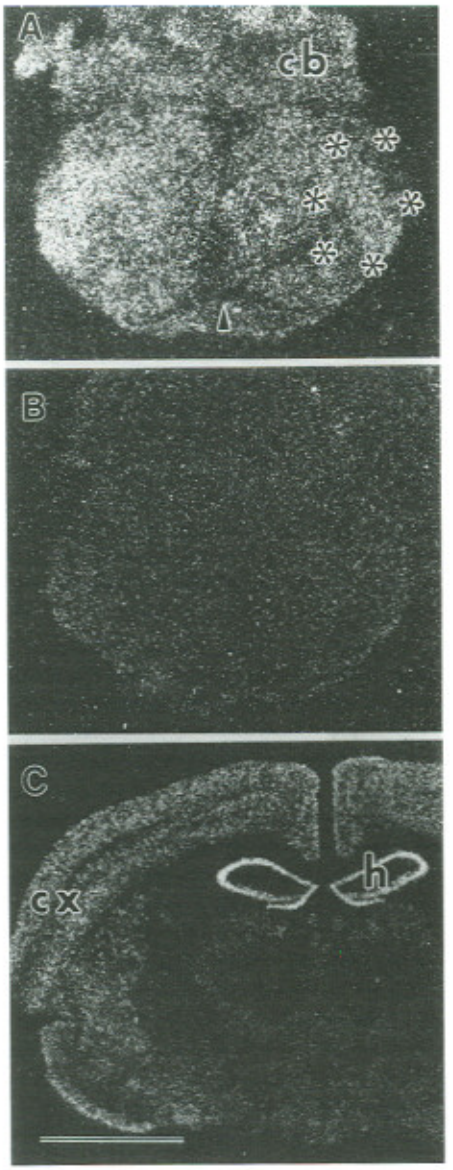

Figure 8. In Situ Hybridization Experiments to Demonstrate that the NMDA Receptor Is Normally Expressed in the Trigeminal Nuclei at the Time of Formation of the Barrelettes

(A) An antisense probe corresponding to 69 bp of the 5′ untranslated region and to the 258 bp coding region for the first 86 amino acids of the NMDAR1 protein was hybridized to coronal sections through the brainstem of a normal control mouse on P0.

(B) A section adjacent to that shown in (A) was hybridized with the sense probe. This section shows no hybridization. The antisense probe, when hybridized to a coronal section through the forebrain of an adult mouse (C), reveals mRNA patterns similar to those published previously by Moriyoshi et al. (1991). cb, cerebellum; cx, cortex. Arrowhead in (A) points to the midline. Asterisks in (A) indicate approximate boundaries of the subnucleus interpolaris. Scale bar, 1 mm in (A) and (B), 2.2 mm in (C).

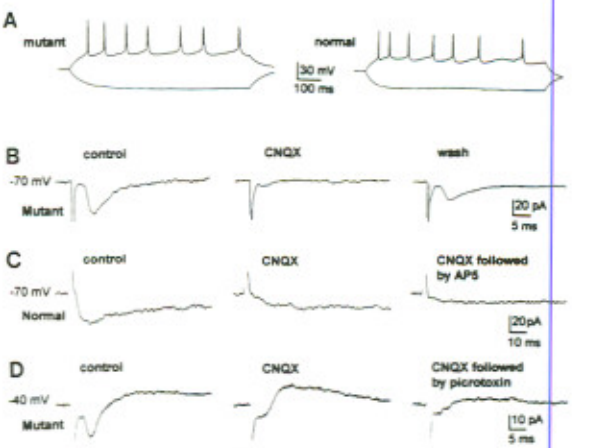

Figure 9. Neuronal Excitability and Synaptic Transmission Are Present in the BSTC of P0 Mutant and Normal Mice

(A) Membrane voltage changes in response to current steps (± 0.04 nA). The depolarizing current step initiated a train of action potentials in both the mutant and normal neurons.

(B) The synaptic current evoked by trigeminal tract stimulation has only non-NMDA receptor–mediated component in the mutant slice. The fast inward current evoked at a holding potential of −70 mV was abolished by CNQX (15 μM) and recovered after subsequent washout of CNQX.

(C) The synaptic current has both NMDA and non-NMDA receptor–mediated components in the normal slice. After application of CNQX (15 μM), a small slow inward current remained and was later abolished by the addition of AP5 (100 μM). Holding potential, −70 mV.

(D) The inhibitory synaptic current was present in the mutant slice. The synaptic current evoked at a holding potential of −40 mV has a fast inward non-NMDA receptor–mediated component and a slow outward $GABA_A$ receptor–mediated component. The latter was blocked by picrotoxin (100 μM).

ral activity, we used whole-cell patch clamp recording. Coronal slices were cut through the BSTC of normal and mutant mice, and the patch electrode was advanced gradually into the trigeminal nuclei of the slice until a cell was encountered and a tight seal was formed between the electrode and cytoplasmic membrane. The concentric bipolar-stimulating electrode was positioned at the lateral margin of the BSTC, where the trigeminal tract is located. Axons coursing through this tract send radially oriented collaterals into the BSTC, where they form terminal arbors. Once into the whole-cell mode by rupturing the membrane, the current clamp was performed. Cells within the whisker representation region of the BSTC were identified as neurons based on their ability to fire fast action potentials in response to depolarizing current pulses (Figure 9A). Cells from both NMDAR1 mutant (n = 8) and normal mice (n = 7) exhibited neuronal excitability at P0.

Under the voltage clamp, electrical stimulation (0.2 to 1 mA) of the trigeminal tract routinely evoked excitatory postsynaptic currents (EPSCs; Figures 9B and 9C). At holding potentials at or negative to the resting potential, synaptic currents were inward going. In mutant slices (n = 3), only a fast inward current was apparent, which was abolished by bath application of 6-cyano-7-nitroquinoxaline-2,3-dione (CNQX), an antagonist for non-NMDA receptors, indicating the absence of NMDA receptor–mediated component (Figure 9B). In wild-type slices (n = 2), there were both fast non-NMDA receptor–mediated (sensitive to CNQX) and slow NMDA receptor–mediated (sensitive to AP5) postsynaptic currents (Figure 9C),

suggesting that the transmission is mediated via glutamate in this pathway.

It is also important to note that inhibitory synaptic currents (IPSCs) were present in some cells. An example of the IPSCs in the mutant slice is shown in Figure 9D (the cell was held at −40 mV). There were an early inward EPSC (blocked by CNQX) and a slow outward going inhibitory current. The IPSC seemed to be mediated by picrotoxin-sensitive $GABA_A$ receptors (n = 1).

Discussion

Studies on the role of NMDA receptors during map formation have focused primarily on the effects of applying NMDA receptor antagonists to projection zones during the time when these zones are being innervated and, in particular, as the afferent arbor is being elaborated. We have used an alternate strategy to explore this issue, that of eliminating the gene that encodes an essential subunit of the NMDA receptor. Our genomic Southern blot analysis showed that *NMDAR1* is a single copy gene in the genome and we have deleted close to half of the protein-coding regions, including four transmembrane domains that are important for the formation of a functional NMDA channel (reviewed by Nakanishi, 1992; Figure 2). Further, results from whole-cell patch clamp recording of brainstem trigeminal neurons in the mutant mice confirmed that we have knocked out NMDA receptor activity (Figure 9B). Our results show that, in the absence of NMDA receptors and in the presence of functional excitatory and inhibitory synaptic transmission, postsynaptic neurons fail to aggregate into barrelettes. We thus conclude that NMDA receptors are involved in the detailed patterning of target neurons, and most likely of afferent axons as well, to reflect the precise arrangement of peripheral sensory organs.

We present several lines of evidence to support this conclusion. First, with the use of CO histochemistry, no whisker-related segmentation is seen in the trigeminal nuclei of the mutant animal at a time when a patchy pattern is clearly discernible in the same regions of littermate controls (Figures 3 and 4). High levels of CO activity are present in trigeminal afferent arbors and their postsynaptic target neurons in the BSTC (Chiaia et al., 1992a, 1992b). Second, immunostaining for CTBP documents that, in the absence of afferent and target cell patterning, extracellular matrix molecules also do not take on a whisker-specific distribution in the hindbrain (Figure 5). Third, immunolabeling with axon-specific antibodies reveals that early events, such as the initial outgrowth of ganglion cell axons to their appropriate peripheral and central targets, occur along a normal schedule (Figure 6). Fourth, the DiI labeling experiments document that trigeminal sensory axons form topographically appropriate connections between the whisker pad and the BSTC (Figure 7). These observations support the notion that the initial targeting, pathfinding, and topographic organization of axon systems can occur without the activation of the NMDA receptor, and that these events are unrelated to activity-dependent mechanisms (for a recent review see Goodman and Shatz, 1993). And, finally, results from the in situ hybridization and electrophysiological studies document that, in normal mice, the NMDAR1 subunit is expressed at high levels in the trigeminal nuclei and forms functional NMDA receptors on the day of birth, the time when the whisker-related patterns have just emerged, inculpating the receptor subunit as a participant in this event.

We do not have direct evidence as to whether the lack of barrelettes in mutant mice is due to a failure of segregation of afferent axon arbors. However, the DiI labeling experiments suggest that while the trigeminal projection is topographically organized in the BSTC, individual axon arbors may be more widespread in mutant animals than in normal littermates (Figure 7B). This is consistent with the hypothesis that NMDA receptor–mediated activity plays a major role in the refinement of axonal projections (reviewed by Constantine-Paton et al., 1990; Shatz, 1990).

Since the mutant animals do not survive beyond P2, one might argue that the lack of pattern formation in the trigeminal nuclei merely reflects a developmental retardation. We think this is unlikely. Since malnutrition leads to retardation of the development of cortical barrels (Vongdokmai, 1980), body weight was monitored for all newborn animals. The average weights of knockout animals were not statistically different from those of normal animals that had undergone the same treatment (e.g., blocked birth, vaginal delivery, litter culling). Second, the anatomical studies show clearly that other morphogenetic events in this system, such as outgrowth of ganglion cell axons and arrival of the axons at the brainstem, occur along a normal schedule. In addition, we have labeled thalamocortical axons to examine the timing of thalamic axon ingrowth into the neocortex: they reach the cortex in mutant mice at the same time as in littermate controls (unpublished data). Furthermore, there is no obvious difference in the laminar organization of the primary somatosensory cortex in mutant and normal mice at P0 (unpublished data). These observations validate our conclusion that the absence of barrelettes in the mutant animals is not due to the general arrest or delay of development, although we cannot completely rule out the possibility that barrelette formation is specifically delayed.

Studies in the visual system have demonstrated that activity plays a critical role in achieving connectional precision between developing cell groups (for reviews see Constantine-Paton et al., 1990; Shatz, 1990). In contrast, studies in which TTX or AP5 was applied to the infraorbital nerve or to the developing somatosensory cortex of rats did not result in blocking the formation of barrel patterns in the somatosensory cortex (Chiaia et al., 1992c; Henderson et al., 1992; Schlaggar et al., 1993). These reports led to the general belief that in the trigeminal system, activity plays a less important role during the development of whisker-related patterns (Katz, 1993a). However, it should be noted that in the above experiments, activity was blocked as of the day of birth. In the BSTC of the rat, the whisker-related pattern is present before the time of birth (Chiaia et al., 1992b) and, in some strains of rats, thalamocortical axons are already patterned on P0 (Schlaggar and O'Leary, 1993; cf. Erzurumlu and Jhaveri, 1990; Blue et al., 1991). Thus, organizational information from the BSTC

may already have been encoded in the developing thalamocortical axons by the time activity or NMDA receptor blockade is initialized. Our results document that in the absence of functional NMDA receptors, barrelettes fail to develop in the hindbrain. Extrapolating from this result, we suggest that the formation of whisker-related patterns (barreloids and barrels) in the thalamus and cortex might also depend on activation of NMDA receptors.

Physiological studies on the receptive fields of individual fetal trigeminal ganglion cells reveal that spontaneous activity is low during the time barrelettes form in the rats (E16–E20), but that the majority of ganglion cells respond to indentation of the skin at the base of a single follicle (Chiaia et al., 1993). It is possible that gentle pressure of the uterine wall could stimulate parts of the whisker pad. Given that peripheral sensory afferents are organized in a whisker-specific pattern before central patterns emerge, summed over time, this could lead to synchronous activation of ganglion cells innervating a single whisker and a consequent whisker-specific patterning of the central afferents and postsynaptic cells via activation of NMDA receptors. Alternatively, it is possible that a low level of spontaneous activity, in combination with coupling among neighboring ganglion cells, brainstem neurons, or both could result in the observed patterns (cf. Katz, 1993b).

Our electrophysiological studies show that in the absence of NMDAR1 protein, NMDA receptor activity is absent in the BSTC of mutant animals (Figure 9B). This is consistent with the results of studies conducted in Xenopus oocytes and transfected human kidney cells (reviewed by Nakanishi, 1992). In addition, we have demonstrated that in the absence of NMDA receptors, brainstem trigeminal neurons are excitable and both excitatory and inhibitory synaptic transmission is functional in the mutants (Figure 9). Thus, sensory inputs from the periphery could be transmitted to and processed in both the mutant and normal BSTC. We hypothesize that failure of the barrelette formation is not caused by the lack of neuronal excitability or of synaptic transmission in the BSTC of NMDAR1 mutants, but by the blockade of the downstream cascade initiated by NMDA receptor activation. For the time being, however, it is not clear whether NMDA receptor inactivation has any modulatory effect on neuronal excitability and synaptic transmission. We are currently carrying out a systematic study of neuronal properties in the mutant mice.

The full sequence of downstream events that occur once the NMDA receptor is activated during the formation of barrelettes is not known. An interesting twist on the activity or NMDA receptor hypothesis is provided by a recent report that shows that prenatal NGF injections interrupt the formation of barrelettes in rats (Henderson et al., 1994). In this context, several studies have provided compelling evidence that NMDA receptor activation may trigger increased neurotrophin synthesis and secretion (Zefra et al., 1991; Amano et al., 1992; Favaron et al., 1993; Gwag et al., 1993; Gwag and Springer, 1993), thus linking activity-dependent refinement to the regulation of trophic factors. Future studies on the developmental expression of neurotrophins and neurotrophic receptors in the BSTC of both knockout and normal pups will shed light on the relationship between NMDA receptor activation and the regulation of neurotrophin expression. Once other factors involved in the signal transduction process downstream of NMDA receptor activation have been identified, these can be deleted using the ES cell technology. We have shown here that the whisker-to-barrel cortex system provides an excellent model for assaying the results of such genetic manipulations on pattern formation in the brain.

Experimental Procedures

Targeting Construct and Transfection of ES Cell

To determine the copy number of *NMDAR1* gene in the mouse genome, genomic DNA isolated from mouse D3 ES cells (Gossler et al., 1986) was digested by BamHI, EcoRI, EcoRV, or HindIII, and hybridized with a probe spanning the region that encodes a 100 amino acid sequence in the carboxy-terminal region of the NMDAR1 protein.

NMDAR1 was cloned from a genomic EMBL3 phage library prepared from D3 ES cells with a probe generated by the polymerase chain reaction (PCR). The targeting construct was prepared by ligating a 2.5 kb XbaI–FspI fragment from the middle part of *NMDAR1*, a 1.8 kb SmaI–XhoI fragment containing a *neo* gene driven by the *pgk* promoter, a 8.3 kb NsiI–XhoI fragment from the 3′ end of *NMDAR1*, and the pBluescript (Stratagene), by digesting with appropriate restriction enzymes. This targeting construct is designed to delete exons 12–19 (Hollmann et al., 1993) and replace them with the *pgk–neo* gene, transcribed in the same orientation.

D3 ES cells were transfected with 50 μg linearized targeting vector by elctroporation (Bio-Rad Gene Pulser set at 800 V and 3.0 μF). G418 selection (100 μg to 150 μg/ml geneticin [GIBCO BRL]) was applied 24 hr after transfection, and resistant clones were isolated after 1 week of selection. Genomic DNA from these clones was digested with EcoRI and probed with a 1.2 kb fragment from the 3′ *NMDAR1*-flanking region (Figure 2B). Positive clones were confirmed by stripping the probe from the membrane and rehybridizing with a 900 bp HindIII–EcoRI probe located in the middle part of *NMDAR1*.

Production of NMDAR1-Mutant Mice

Generation of chimeric mice was done according to the procedure of Bradley (1987). Germline transmission was screened by mating chimeras with C57BL/6 mice and confirmed by genomic Southern blot analysis of tail DNA. Mice heterozygous for the mutation were interbred to homozygozity. Germline chimeras were backcrossed with 129/Sv, BALB/c, and C57BL/6 to transfer the mutation into these inbred lines.

Heterozygous females were mated overnight with the heterozygous males. The following morning, the females were checked for a vaginal plug and, if present, this day was referred to as E0. Plugged females usually gave birth between E18.5 and E19.5. To delay birth, pregnant mothers were injected with terbutaline (5 mg/kg) every 4 to 6 hr, starting on E18.5. This usually delayed birth for an additional day. Treated animals were then allowed to give birth. Newborn pups were weighed and put into an air incubator (55% humidity, 34°C). They were then monitored every 1–2 hr. If cyanosis was observed, they were treated in a chamber for 5 min with 5% CO_2 and 20% O_2 balanced with N_2. About 15–25 hr after birth, the pups were overdosed with anesthetics and perfused with saline followed by 4% paraformaldehyde in phosphate buffer.

Genotyping of the mice was initially done by Southern blotting of tail DNA; later mice were typed by PCR analysis with a set of *neo1* primers (5′-GCTTGGGTGGAGAGGCTATTC and 5′-CAAGGTGAGATGACAGGAGATC, 280 bp PCR product) and a set of primers to the deleted region of the mutant *NMDAR1* allele (5′-TGACCCTGTCCTCTGCCATG and 5′-GCTTCTCCATGTGCCGGTAC, 550 bp PCR product).

Histochemical Methods

Cytochrome oxidase histochemistry was performed according to the procedure described by Wong-Riley (1979). Aldehyde-fixed cryoprotected brainstems were cut into 50 μm thick sections in the coronal plane on a freezing microtome. Sections were collected in phosphate buffer, and incubated in a solution consisting of 4 g sucrose, 50 mg diaminobenzidine, and 40 mg cytochrome C in 100 ml phosphate

buffer at 37°C in the dark, until a golden brown reaction product could be visualized. The sections were rinsed in phosphate buffer, mounted onto slides, coverslipped with glycerol, and examined under a microscope.

For axonal labeling along the trigeminal pathway, small crystals of the carbocyanine dye DiI (Godement et al., 1987; Molecular Probes) were placed in rows A and E on one side of the face and in row C on the other side of aldehyde-fixed E17 and P0 mouse heads. Specimens were stored in the fixative at 37°C for 3–8 weeks to allow for dye diffusion. The brainstems were dissected out, embedded in agar, and sectioned on a vibratome at a thickness of 100 μm. The sections were mounted onto slides, coverslipped with phosphate buffer, and viewed under epifluorescence using a rhodamine filter.

Immunohistochemistry for CTBP and β-tubulin was carried out according to published protocols (Crossin et al., 1989; Jhaveri et al., 1991; Easter et al., 1993). In brief, 50 μm of brainstem sections was collected in PBS and preincubated in PBS plus 5% normal goat serum for 30 min at room temperature. The sections were then incubated overnight at room temperature in rabbit anti-mouse CTBP (dilution 1:50) or TuJ1 antibody (dilution 1:2000) in PBS plus 0.1%NaN_3 plus 5% normal goat serum. Control sections were incubated in preimmune serum. The sections were rinsed three times with PBS and incubated in FITC-conjugated goat anti-rabbit secondary antibody (for CTBP) or in FITC-conjugated goat anti-mouse secondary antibody (for TuJ1) for 2 hr at room temperature. Following three rinses in phosphate buffer, sections were mounted onto slides, coverslipped with DPX mountant, and viewed under epifluorescence using an FITC filter.

In Situ Hybridization

In situ hybridization was done according to Whitfield et al. (1990) on frozen 12 μm sections of both P0 and adult mouse brains. ^{35}S-labeled RNA probes were generated in both transcription directions by using a subclone in the Bluescript vector (Stratagene) containing cDNA corresponding to 69 bp of the 5′ untranslated region and 258 bp coding region for the first 86 amino acids of the NMDAR1 protein.

Electrophysiological Recording

Animals (P0) were decapitated under Metofane anesthesia, the brain was removed rapidly and placed in ice-cold oxygenated artificial cerebrospinal fluid composed of the following: 119 mM NaCl, 2.5 mM KCl, 1.3 mM $MgCl_2$, 2.5 mM $CaCl_2$, 26 mM $NaHCO_3$, 1 mM NaH_2PO_4, 10 mM glucose (pH 7.4). Coronal slices, 500 μm thick, were cut with a vibratome through the brainstem, then maintained in an incubation chamber for at least 1 hr at room temperature (22°C–25°C). For recording experiment, a slice was transferred to a submerge-recording chamber, where it was held by a nylon net and constantly perfused with oxygenated artificial cerebrospinal fluid (95% O_2 and 5% CO_2). The brainstem trigeminal nuclei and trigeminal fiber tract were visualized under a dissecting microscope.

Whole-cell recordings were obtained with conventional patch techniques. Patch electrodes (4–8 MΩ) were fabricated from soft glass (Drummond), and pulled on a three-step puller (Sutter Instrument). The internal solution contained 90 mM K acetate, 20 mM KCl, 2 mM $MgCl_2$, 3 mM EGTA, 40 mM HEPES, 1 mM $CaCl_2$, 2 mM ATP–Mg, and 0.2 mM GTP–Li (pH 7.2). Once into the whole-cell mode, current injection experiments were first performed under the current clamp. Resting membrane potentials ranged from −45 to −65 mV. A constant holding current was used to keep the resting potential at −60 mV if necessary. Synaptic currents were then recorded under the voltage clamp. Trigeminal fibers were stimulated by a concentric bipolar electrode (Rhodes Instrument) that delivered 0.1 ms pulses. Data were digitized, stored, and analyzed on a 486 computer with an analog to digital converter (Digidata) and pCLAMP program (both by Axon Instrument). Signals were filtered at 2 KHz. Synaptic current records shown in Figure 9 were the average of six traces sampled at an interval of 20 s. Drugs were applied via bath application at final concentrations of 15 μM CNQX (Tocris Neuramin), 100 μM AP5 (Tocris Neuramin), or 100 μM picrotoxin (Sigma).

Acknowledgments

We wish to thank Drs. K. Crossin, A. Frankfurter, R. Kemler, M. Rudnicki, and A. J. Silva for their gift of various reagents; S. Hsu, W. Lin, and E. Golland for technical assistance; Drs. L. Van Kaer and A. J. Silva for help with ES cell work; Drs. P. G. Ashton-Rickardt and E. Li for the advice on making chimeras; Dr. B. Kosofsky for help with in situ hybridization; Dr. D. G. Rainnie for advice on brainstem recording; Drs. M. Sur and J. Schneider for critical reading of the manuscript; and the members of Tonegawa lab for helpful discussion and encouragement. Y. L. and C. C. are research associates of the Howard Hughes Medical Institute. This work was funded by the Howard Hughes Medical Institute (S. T.), the Shionogi Institute for Medical Science (S. T.), and by a grant from the National Institutes of Health (NS 27678) to S. J.

Received December 6, 1993; revised December 29, 1993.

References

Amano, T., Yamakuni, T., Okabe, N., Kuwahara, R., Ozawa, F., and Hishinuma, F. (1992). Regulation of nerve growth factor and nerve growth factor receptor production by NMDA in C6 glioma cells. Mol. Brain Res. *14*, 35–42.

Bates, C. A., and Killackey, H. P. (1985). The organization of the neonatal rat's brainstem trigeminal complex and its role in the formation of central trigeminal patterns. J. Comp. Neurol. *240*, 265–287.

Bear, M. F., Kleinschmidt, A., Gu, Q., and Singer, W. (1990). Disruption of experience-dependent synaptic modification in striate cortex by infusion of an NMDA receptor antagonist. J. Neurosci. *10*, 909–925.

Belford, G. R., and Killackey, H. P. (1979). Vibrissae representation in subcortical trigeminal centers of the neonatal rat. J. Comp. Neurol. *183*, 305–322.

Belford, G. R., and Killackey, H. P. (1980). The sensitive period in the development of the trigeminal system of the neonatal rat. J. Comp. Neurol. *193*, 335–350.

Blue, M. E., Erzurumlu, R. S., and Jhaveri, S. (1991). A comparison of pattern formation by thalamocortical and serotonergic afferents in the rat barrel field cortex. Cerebral Cortex *1*, 380–389.

Bradley, A. (1987). Production and analysis of chimeric mice. In Teratocarcinomas and Embryonic Stem Cells: A Practical Approach, E. J. Robertson, ed. (Oxford: IRL Press), pp. 113–151.

Capecchi, M. R. (1989). Altering the genome by homologous recombination. Science *244*, 1288–1292.

Chiaia, N. L., Bennett-Clarke, C. A., Eck, M., White, F. A., Crissman, R. S., and Rhoades, R. W. (1992a). Evidence for prenatal competition among the central arbors of trigeminal primary afferent neurons. J. Neurosci. *12*, 62–76.

Chiaia, N. L., Bennett-Clarke, C. A., and Rhoades, R. W. (1992b). Differential effects of peripheral damage on vibrissa-related patterns in trigeminal nucleus principalis, subnucleus interpolaris, and subnucleus caudalis. Neuroscience *49*, 141–156.

Chiaia, N. L., Fish, S. E., Bauer, W. R., Bennett-Clarke, C. A., and Rhoades, R. W. (1992c). Postnatal blockade of cortical activity by tetrodotoxin does not disrupt the formation of vibrissae-related patterns in the rat's somatosensory cortex. Dev. Brain Res. *66*, 244–250.

Chiaia, N. L., Bauer, W. R., and Rhoades, R. W. (1993). Prenatal development of the receptive fields of individual trigeminal ganglion cells in the rat. J. Neurophysiol. *69*, 1171–1180.

Cline, H. T., Debski, E., and Constantine-Paton, M. (1987). NMDA receptor antagonist desegregates eye-specific stripes. Proc. Natl. Acad. Sci. USA *84*, 4342–4345.

Constantine-Paton, M., Cline, H. T., and Debski, E. (1990). Patterned activity, synaptic convergence, and the NMDA receptor in the developing visual pathways. Annu. Rev. Neurosci. *13*, 129–154.

Crossin, K. L., Hoffman, S., Tan, S. S., and Edelman, G. M. (1989). Cytotactin and its proteoglycan ligand mark structural and functional boundaries in somatosensory cortex of the early postnatal mouse. Dev. Biol. *136*, 381–392.

Durham, D., and Woolsey, T. A. (1984). Effects of neonatal whisker lesions on mouse central trigeminal pathways. J. Comp. Neurol. *223*, 424–447.

Easter, S. S., Jr., Ross, L. S., and Frankfurter, A. (1993). Initial tract formation in the mouse brain. J. Neurosci. *13*, 285–299.

Erzurumlu, R. S., and Jhaveri, S. (1990). Thalamic axons confer a blueprint of the sensory periphery onto the developing rat somatosensory cortex. Dev. Brain Res. *56*, 229–234.

Erzurumlu, R. S., and Jhaveri, S. (1992). Trigeminal ganglion cell processes are spatially ordered prior to the differentiation of the whisker pad. J. Neurosci. *12*, 3946–3955.

Favaron, M., Manev, R. M., Rimland, J. M., Candeo, P., Beccaro, M., and Manev, H. (1993). NMDA-stimulated expression of BDNF mRNA in cultured cerebellar granule neurons. Neuroreport *4*, 1171–1174.

Godement, P., Vanselow, J., Thanos, S., and Bonhoeffer, F. (1987). A study of developing visual systems with a new method for staining neurons and their processes in fixed tissue. Development *101*, 697–913.

Goodman, C. S., and Shatz, C. J. (1993). Developmental mechanisms that generate precise patterns of neuronal connectivity. Cell/Neuron, *72/10* (Suppl.), 77–98.

Gossler, A., Doetschman, T., Korn, R., Serfling, E., and Kemler, R. (1986). Transgenesis by means of blastocyst-derived embryonic stem cell lines. Proc. Natl. Acad. Sci. USA *83*, 9065–9069.

Gwag, B. J., Sessler, F. M., Waterhouse, B. D., and Springer, J. E. (1993). Regulation of nerve growth factor mRNA in the hippocampal formation: effects of N-methyl-D-aspartate receptor activation. Exp. Neurol. *121*, 160–171.

Gwag, B. J., and Springer, J. E. (1993). Activation of NMDA receptors increases brain-derived neurotrophic factor (BNDF) mRNA expression in the hippocampal formation. Neuroreport *5*, 125–128.

Hahm, J.-O., Langdon, R. B., and Sur, M. (1991). Disruption of retinogeniculate afferent segregation by antagonists to NMDA receptors. Nature *351*, 568–570.

Henderson, T. A., Woosley, T. A., and Jacquin, M. F. (1992). Infraorbital nerve blockade from birth does not disrupt central trigeminal pattern formation in the rat. Dev. Brain Res. *66*, 146–152.

Henderson, T. A., Rhoades, R. W., Bennett-Clarke, C. A., Osborne, P. A., Johnson, E. M., Jr., and Jacquin, M. F. (1993). NGF augmentation rescues trigeminal ganglion and principalis neurons, but not brainstem or cortical whisker patterns, after infraorbital nerve injury at birth. J. Comp. Neurol. *336*, 243–260.

Henderson, T. A., Johnson, E. M., Jr., Osborne, P. A., and Jacquin, M. F. (1994). Fetal NGF augmentation preserves excess trigeminal ganglion cells and interrupts whisker-related pattern formation. J. Neurosci., in press.

Hollmann, M., Boulter, J., Maron, C., Beasley, L., Sullivan, J., Pecht, G., and Heinemann, S. (1993). Zinc potentiates agonist-induced currents at certain splice variants of the NMDA receptor. Neuron *10*, 943–954.

Jeanmonod, D., Rice, F. L., and Van der Loos, H. (1981). Mouse somatosensory cortex: alterations in the barrelfield following receptor injury at different early postnatal ages. Neuroscience *6*, 1503–1535.

Jhaveri, S., Erzurumlu, R. S., and Crossin, K. (1991). Barrel construction in rodent neocortex: role of thalamic afferents versus extracellular matrix molecules. Proc. Natl. Acad. Sci. USA *88*, 4489–4493.

Jhaveri, S., and Erzurumlu, R. S. (1992). Two phases of pattern formation in the developing rodent trigeminal system. In Development of the Central Nervous System in Vertebrates, S. C. Sharma and A. M. Goffinet, eds. (New York: Plenum Press), pp. 167–178.

Katz, L. C. (1993a). Cortical space race. Nature *364*, 578–579.

Katz, L. C. (1993b). Coordinate activity in retinal and cortical development. Curr. Opin. Neurobiol. *3*, 93–99.

Kleinschmidt, A., Bear, M. F., and Singer, W. (1987). Blockade of NMDA receptors disrupts experience-dependent modifications in kitten striate cortex. Science *238*, 355–358.

Ma, P. M. (1991). The barrelettes: Architectonic vibrissal representations in the brainstem trigeminal complex of the mouse. I. Normal structural organization. J. Comp. Neurol. *309*, 161–199.

Ma, P. M. (1993). Barrelettes: Architectonic vibrissal representations in the brainstem trigeminal complex of the mouse. II. Normal postnatal development. J. Comp. Neurol. *327*, 376–397.

Ma, P. M., and Woolsey, T. A. (1984). Cytoarchitectonic correlates of the vibrissae in the medullary trigeminal complex of the mouse. Brain Res. *306*, 374–379.

Moriyoshi, K., Masu, M., Ishii, T., Shigemoto, R., Mizuno, N., and Nakanishi, S. (1991). Molecular cloning and characterization of the rat NMDA receptor. Nature *354*, 31–37.

Nakanishi, S. (1992). Molecular diversity of glutamate receptors and implications for brain function. Science *258*, 597–603.

Schlaggar, B. L., and O'Leary, D. D. M. (1993). Patterning of the barrel field in somatosensory cortex with implications for the specification of neocortical areas. Perspect. Dev. Neurobiol. *1*, 81–92.

Schlaggar, B. L., Fox, K., and O'Leary, D. D. M. (1993). Postsynaptic control of plasticity in developing somatosensory cortex. Nature *364*, 623–626.

Shatz, C. J. (1990). Impulse activity and the patterning of connections during CNS development. Neuron *5*, 745–756.

Simon, D. K., Prusky, G. T., O'Leary, D. D. M., and Constantine-Paton, M. (1992). N-methyl-D-aspartate receptor antagonists disrupt the formation of a mammalian neural map. Proc. Natl. Acad. Sci. USA *89*, 10593–10597.

Stainier, D. Y. R., and Gilbert, W. (1990). Pioneer neurons in the mouse trigeminal sensory system. Proc. Natl. Acad. Sci. USA *87*, 923–927.

Van der Loos, H., and Welker, E. (1985). Development and plasticity of somatosensory brain maps. In Development and Plasticity of Somatosensory Brain Maps, M. Rowe and W. D. Willis, Jr., eds. (New York: Alan R. Liss), pp. 53–67.

Vongdokmai, R. (1980). Effect of protein malnutrition on development of mouse cortical barrels. J. Comp. Neurol. *191*, 283–294.

Whitfield, H. J., Jr., Brady, L. S., Smith, M. A., Mamalaki, E., Fox, R. J., and Herkenham, M. (1990). Optimization of cRNA probe in situ hybridization methodology for localization of glucocorticoid receptor mRNA in rat brain: a detailed protocol. Cell. Mol. Neurobiol. *10*, 145–157.

Wong-Riley, M. (1979). Changes in the visual system of monocularly sutured or enucleated cats demonstrable with cytochrome oxidase histochemistry. Brain Res. *171*, 11–28.

Woolsey, T. A. (1990). Peripheral alteration and somatosensory development. In Development of Sensory Systems in Mammals, E. J. Coleman, ed. (New York: Wiley), pp. 461–516.

Zefra, F., Castren, E., Thoenen, H., and Lindholm, D. (1991). Interplay between glutamate and γ-aminobutyric acid transmitter systems in the physiological regulation of brain-derived neurotrophic factor and nerve growth factor synthesis in hippocampal neurons. Proc. Natl. Acad. Sci. USA *88*, 10037–10041.